

Density extraction from P-wave AVO inversion: Tuscaloosa Trend example

Jyoti Behura¹, Nurul Kabir², Richard Crider², Petr Jilek², and Ellen Lake³

¹Center for Wave Phenomena, Colorado School of Mines, Golden, Colorado 80401, USA; ²BP Exploration and Production Technology Group, Houston, Texas 77079, USA; ³BP North American Gas Strategic Performance Unit, Houston, Texas 77079, USA.

Summary

Density extraction from AVO inversion is thought to be unstable and difficult. Recent research has, however, shown that it is possible to extract density reliably from P-wave reflection data if the density contrast is significant across the interface. This approach is tested over a gas reservoir where petrophysical evidence suggests that density is the primary driver of reflectivity. By adopting a linear as well as a non-linear approach, inversion is performed for density and P-wave velocity from a 3D prestack seismic dataset acquired over this gas reservoir. The non-linear inversion results agree well with the log and production data, thus proving that density can be extracted reliably in this case and used for reservoir characterization. We use the extracted density along with the P-wave velocity to distinguish the low-density porous gas sands from wet sands, tight sands, and shales.

Introduction

The Tuscaloosa Trend, located in South Louisiana, is a series of gas fields. All these sands are of Cretaceous age and were deposited in a near-shore marine depositional environment. Data from a 3D seismic survey over this area is used in this study. Lithology at the reservoir depths consists of gas-saturated sands along with wet sands, tight sands, and shales. Reduction of drilling risk and optimization of production requires delineating and separating gas sands from other lithologies.

Amplitude-variation-with-offset (AVO), a useful tool in seismic exploration, is applied here to extract physical parameters (P-wave velocity, S-wave velocity, and density) used for lithology discrimination. In isotropic media, P-wave AVO is a function of four quantities: g (background V_P/V_S), P-wave velocity contrast, S-wave velocity contrast, and density contrast across the interface. However, a common impression is that these individual parameters cannot be found uniquely using this tool i.e. all these parameters cannot be decoupled from one another using AVO without long-offset data. Estimation of density can be particularly difficult (Debski and Tarantola, 1995) and requires wide range of incidence angles to be stable as pointed out by Li (2005). Kabir et. al. (2006), however, showed that density can be estimated reliably from near- and mid-offsets where density contrast is the dominant contributing factor in the AVO equation (Figure 1). Through a field data example, they could successfully relate the estimated density to gas saturation in the Ma-

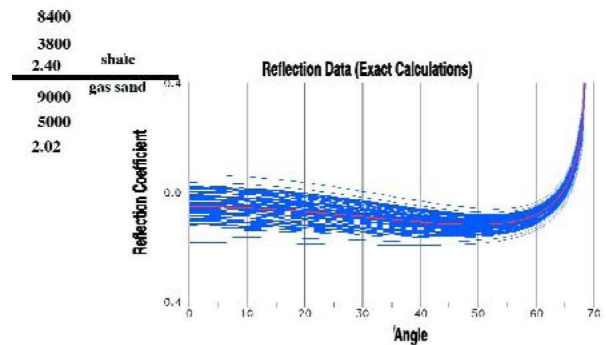


Fig. 1: Sensitivity curves for the density parameter generated by varying the density of the bottom layer between +20% and -20% (Kabir et. al. 2006).

hogany gas field in offshore Trinidad. The same idea is expressed by Li (2005) who concludes that, “In general, high porosity reservoirs and reservoirs with better density contrasts or anomalies are appropriate candidates for applying density inversion.”

The prestack data in this Tuscaloosa Trend study, however, spans from 0° to 30°. So the obvious question is whether density can be reliably extracted in this field using only near- to mid-offset data. In other words, is density the primary driver of reflectivity in this reservoir?

Why density?

To test the applicability of density inversion, well logs are analyzed for one of the Tuscaloosa fields. A cross-plot of the density and P-wave slowness logs (inverse of P-wave velocity) in one of the wells is shown in Figure 2a, where the data points have been scaled by the corresponding gamma ray recording at that depth. Note that the density of most of the sands is quite different from that of the shales. On the other hand, the P-wave velocities of sands and shales span over the same range. By knowing densities, sands can be separated from shales, which is not possible using P-wave velocities alone. So we conclude that density is the primary driver of reflectivity between gas sands and shales in this area.

From Figure 2b, in conjunction with Figure 2a, also note that the low density and low P-wave velocity sands are the producing gas sands (with the low density resulting from high porosity). With increasing water saturation, the density and velocity of these porous sands increases.

Density from P-wave AVO inversion

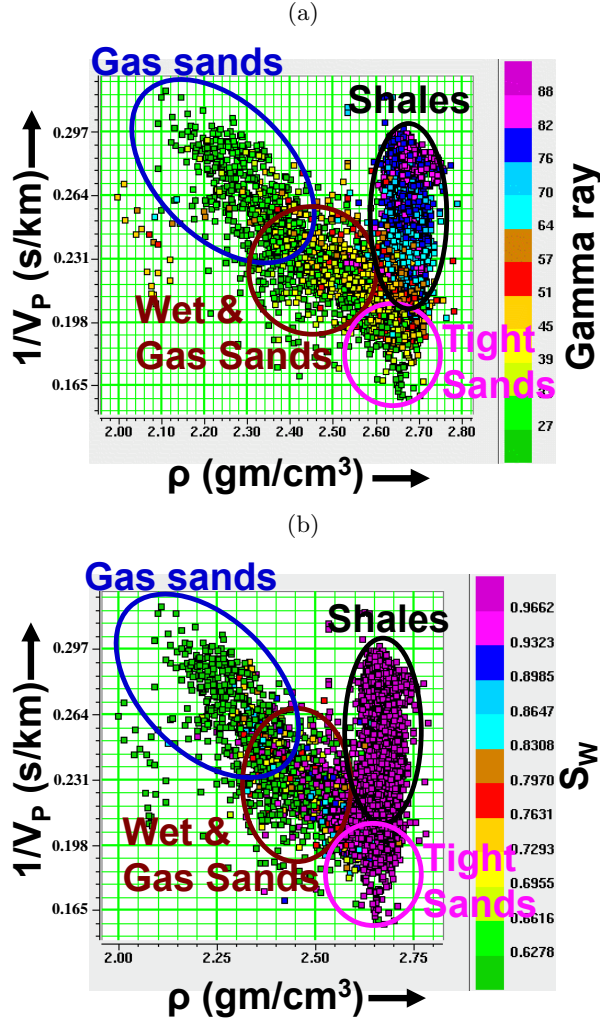


Fig. 2: Crossplots of P-wave slowness and density scaled by (a) gamma ray and (b) water saturation from one of the wells in the study area.

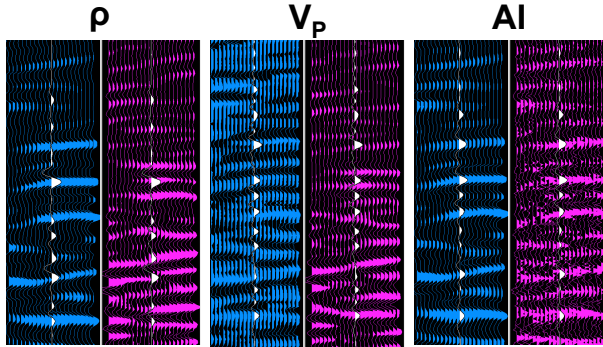


Fig. 3: Comparison of performance of non-linear (blue) and linear (magenta) inversions for density (left panel), P-wave velocity (middle panel), and acoustic impedance (right panel). White curves represent synthetics calculated from well logs.

Tight sands have the highest density and velocity amongst them all. The conclusion from the above analysis is that density can not only help distinguish sands from shales, but also, in combination with P-wave velocity, might help separate gas sands from wet and tight sands. Separating gas sands from shales and tight sands would be relatively easy; separating gas sands from wet sands would be more challenging as evident from the overlap in properties of the two (Figures 2a and 2b).

Linear vs. non-linear inversion

A similar procedure is adopted as Kabir et. al. (2006) to separate gas sands from wet sands, tight sands, and shales using density extracted from near-to-mid angle ($0^\circ - 30^\circ$) AVO. Both linear and a non-linear inversion algorithms are used to compare their performance. Conventional linearized approximations of P-wave AVO (e.g. Smith and Gidlow, 1987) are valid only for small contrasts in rock properties across the interface. For non-linear inversion, Lavaud et. al. (1999) reparameterized the Knott-Zoeppritz equation in terms of a background parameter and three contrast parameters as:

$$R_{PP}(\theta) = f(\chi, e_P, e_S, e_\rho), \quad (1)$$

where

$$\chi = 2\bar{\beta}^2/\bar{\alpha}^2, \quad (2)$$

$$e_P = (\alpha_2^2 - \alpha_1^2)/(\alpha_2^2 + \alpha_1^2), \quad (3)$$

$$e_S = (\beta_2^2 - \beta_1^2)/(\beta_2^2 + \beta_1^2), \quad (4)$$

$$e_\rho = (\rho_2 - \rho_1)/(\rho_2 + \rho_1), \quad (5)$$

$$1/\bar{\alpha}^2 = (1/\alpha_1^2 + 1/\alpha_2^2)/2, \quad (6)$$

$$1/\bar{\beta}^2 = (1/\beta_1^2 + 1/\beta_2^2)/2, \quad (7)$$

with subscripts 1 and 2 corresponding to the incidence and reflecting half-spaces respectively. The above parametrization imposes no limitations on the magnitude of the contrast parameters and is valid for long-offset data and this parameterization is used for the non-linear inversion here. Because non-linear inversion is based on the exact AVO equation, it is likely to yield more accurate results than linear inversion. For the same reason individual parameters are better resolved, even though this inversion is more computer intensive. Non-linear inversion, however, can be more unstable compared to linear inversion and its solution might get trapped in a local minima (thus yielding the wrong result). The objective function used by this non-linear algorithm is the least-squares error between the observed and computed data (l^2 -norm). Detailed mathematical formulation of the algorithm is given in Lavaud et. al. (1999).

A comparison between the two inversions is shown in Figure 3. The white curves represent synthetics calculated

Density from P-wave AVO inversion

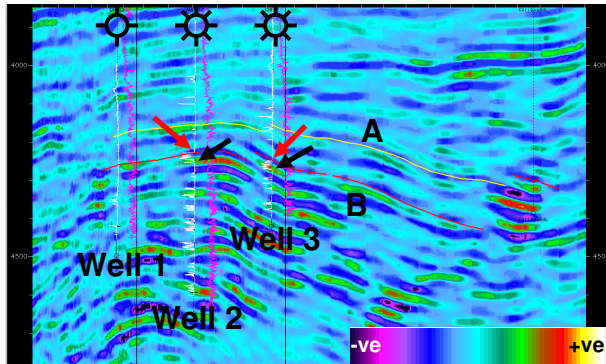


Fig. 4: Density-contrast section from non-linear inversion. Two horizons A and B are marked in yellow and red respectively, along with a dry and two producing wells. Hot colors represent positive contrast while cool colors represent negative contrasts. The density log is shown in white and the P-wave velocity log is shown in magenta.

by computing contrasts in the individual parameters from the well logs and then convolving them with a wavelet. Note the good match between the log curves and the non-linear inversion results for all the three parameters. On the other hand, linear inversion does not show a good match with the log curves, especially for P-wave velocity. The conclusion is that non-linear inversion performs better than linear inversion in this case. From now on, only the non-linear inversion results will be discussed.

Non-linear inversion results

Figure 4 shows the density-contrast section obtained from non-linear inversion. Note that this is a contrast section, not a layer-parameter section; this section only shows if there is a contrast in density across an interface between two layers. The two red arrows are pointing to locations where the density is decreasing with depth (as seen on the density logs shown in white). This implies that there is a negative density contrast. This matches well with the inverted contrast section where the inversion shows a blue region implying a density decrease. The same can be seen at locations pointed out by the two black arrows. Here the density increases from low values to high values and the corresponding positive contrast is seen as a green/red region on the inversion.

To find layer properties, colored inversion is performed on the inverted contrast sections. Colored inversion involves computing an operator using contrast volumes and well logs followed by application of that operator on the whole contrast volume to obtain layer properties (Lancaster and Whitcombe, 2000). Figure 5a shows the interval density of layers obtained after colored inversion. Note the good match between the density log in white and the inversion result. Look at two locations marked by arrows. The logs show low density values which are in agreement with the inversion. Near Well 1, the inversion shows a high density body just below the B horizon, which cannot be a porous sand according to our petrophysical analysis. This agrees

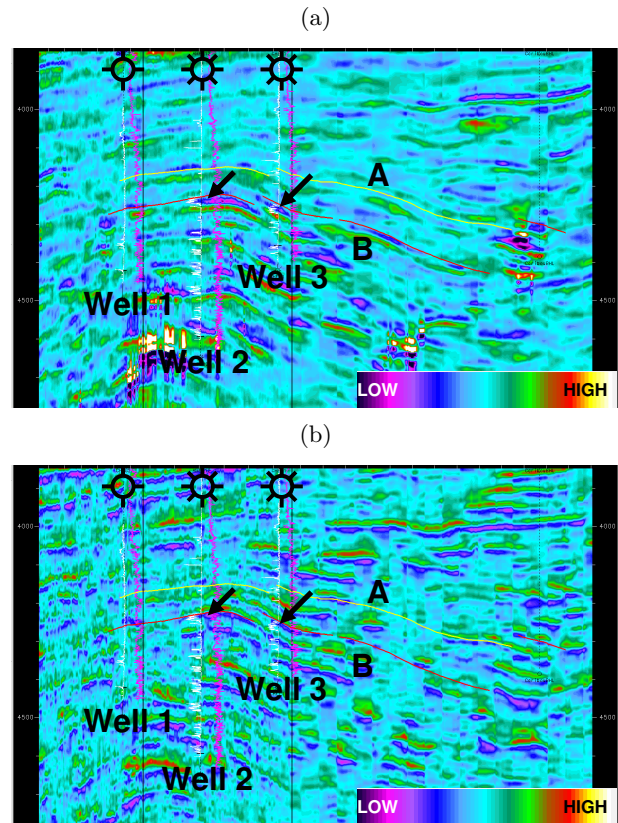


Fig. 5: (a) Density and (b) P-wave velocity sections after colored inversion. Hot colors represent high values while cool colors represent low values. The density log is shown in white and the P-wave velocity log is shown in magenta.

with the drilling and production results. Wells 2 and 3 are good producers as they pass through low density bodies (implying porous sands) while Well 1 is a dry hole with nonporous sands.

The inverted P-wave velocity after colored inversion is shown in Figure 5b. Note that the same locations (marked by arrows) as in the density section above, have low P-wave velocities. According to the petrophysical analysis, these should be porous gas sands which again agrees with the drilling and production results.

Figure 6a is the density map extracted for the B sand. The gas field in this area is trapped on a large faulted structural high. The beds are predominantly dipping to the north and northwest as seen from the contours. The best B production is found on the northeast side of the structure where there is a substantial correlation to the low density areas shown on the extracted density map. Wells 2 and 3 both lie in these low density areas. The low density anomalies on the east and west sides of the field (denoted by the white arrows), probably imply porous sands, but these areas do not have any well penetrations.

The combination of low density and low P-wave veloc-

Density from P-wave AVO inversion

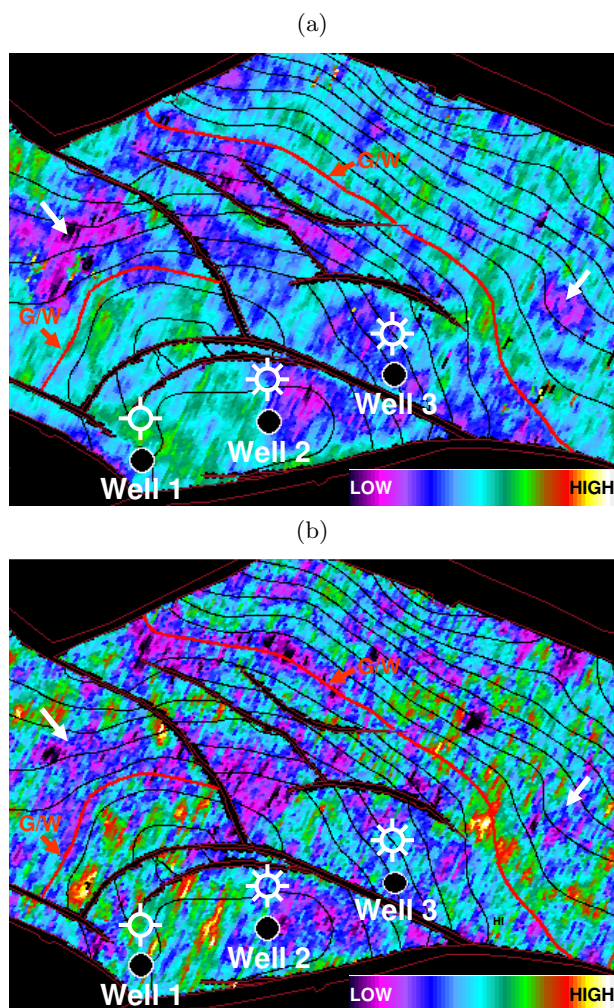


Fig. 6: (a) Density and (b) P-wave velocity maps extracted for B sand. Hot colors represent high values while cool colors represent low values. The contours shown in red denote the approximate gas/water contact for the B horizon.

ity has the highest probability of being a productive gas sand. For the highly productive portion of the B horizon, there are low velocity regions (Figure 6b) which overlie low density regions. The two productive wells (Wells 2 and 3) lie in low P-wave velocity regions while the dry hole (Well 1) is in the high P-wave velocity region. The cumulative production from the B horizon in the Well 2 fault block is 57 bcf. The cumulative production in the Well 3 fault block is 139 bcf. This can be contrasted with the western fault block which has both substantially high density and high P-wave velocities; this block has only produced 2.4 bcf of gas. For the low density anomalies noted earlier on the east and west sides of the field, there are no distinct features on the P-wave map. At some locations, the P-wave velocity is high while at others it is low. For this low density and erratic velocity, the fluid properties for these anomalies cannot be accurately determined.

Because these areas are both structurally low to the gas-water contacts in the field, the sands are undoubtedly wet here.

Discussion

Even though density inversion was successful in this field, this technique should not be blindly applied to all areas. Care should be taken while interpreting the results as a mismatch was observed at one well located outside of the field. The well passes through a thick wet sand but inversion results show a high density region. The thick sand zone has many interbedded shales and thus interference of reflections and tuning might be yielding the wrong inversion results. It is also possible that this contradictory result may have several other explanations: the data might not have been zero-phased at the well, the inversion might be trapped in a local minima, violation of certain assumptions like absence of attenuation, anisotropy etc. More analysis needs to be done to understand the cause of this mismatch. The important lesson is to be careful while interpreting results and geological information and other evidence should be taken into account to improve the chances of success.

Conclusions

Density is the primary driver of reflectivity in this field. Petrophysical analysis suggests that porous gas sands have low density and low P-wave velocity. Porous sands can easily be distinguished from shales and tight sands, but separating gas sands from wet sands is more challenging. Because gas sands have higher porosity and thus lower density than other lithologies, density information can help in locating them, especially when coupled with other geological and structural data. Density extracted from prestack AVO data shows a good match with log and production data and thus AVO inversion for density works well. Moreover, non-linear inversion produced better results than linear inversion in this case and so this should be the preferred methodology. The extracted density and P-wave velocity helped identify gas sands in the field as seen from the good correlation between the interpretation and the log and production data in the field.

Acknowledgments

We are grateful to BP for permission to publish this paper. We also thank SEI (Seismic Exchange, Inc.) for providing the seismic data. The seismic data is owned or controlled by Seismic Exchange, Inc.; the interpretation is that of BP.

Density from P-wave AVO inversion

References

- Debski, W., and A. Tarantola, 1995, Information on elastic parameters obtained from the amplitudes of reflected waves: *Geophysics*, **60**, 1426-1436.
- Kabir, N., R. Crider, R. Ramkhelawan, and C. Baynes, 2006, Can hydrocarbon saturation be estimated using density contrast parameter?: *CSEG Recorder*, 31-37.
- Lancaster, S., and D. Whitcombe, 2000, Fast-track 'colored' inversion: 70th Annual International Meeting, SEG, Expanded Abstracts, **19**, 1572-1575.
- Lavaud, B., N. Kabir, and G. Chavent, 1999, Pushing AVO inversion beyond linearized approximation: *J. Seis. Expl.*, **8**, 279-302.
- Li, Y., 2005, A study on applicability of density inversion in defining reservoirs: 75th Annual International Meeting, SEG, Expanded Abstracts, **24**, 1646-1649.
- Smith, G., and P. Gidlow, 1987, Weighted stacking for rock property estimation and detection of gas: *Geophysical Prospecting*, **35**, 993-1014.